On the Interaction of Ionic Detergents with Lipid Membranes. Thermodynamic Comparison of *n*-Alkyl-$^{+}N(CH_3)_3$ and *n*-Alkyl-SO_4^-

Andreas Beck, Xiaochun Li-Blatter, Anna Seelig, and Joachim Seelig*

Biozentrum, University of Basel, Division of Biophysical Chemistry, Klingelbergstrasse 50/70, CH-4056 Basel, Switzerland

Received: July 29, 2010; Revised Manuscript Received: October 12, 2010

Ionic detergents find widespread commercial applications as disinfectants, fungicides, or excipients in drug formulations and cosmetics. One mode of action is their ease of insertion into biological membranes. Very little quantitative information on this membrane-binding process is available to date. Using isothermal titration calorimetry (ITC) and dynamic light scattering (DLS), we have made a systematic comparison of the binding of cationic and anionic detergents to neutral and negatively charged lipid membranes. The detergents investigated were *n*-alkyl chains carrying either the trimethylammonium chloride ($-^{+}N(CH_3)_3Cl^-$) or the sodium sulfate ($-SO_4^-Na^+$) headgroup with chain lengths of $n = 10-16$. The titration of lipid vesicles into detergent solutions provided the binding enthalpy and the binding isotherm in a model-independent manner. At 25 °C the membrane binding enthalpies, ΔH^0_{mem}, were small (−0.4 to −4.2 kcal/mol) and showed little correlation with the length of the alkyl chains. The ITC binding isotherms were analyzed in terms of a surface partition model. To this purpose, the surface concentration, c_M, of detergent immediately above the plane of binding was calculated with the Gouy−Chapman theory. The surface concentration corrects for electrostatic attraction or repulsion and can be larger or smaller than the bulk detergent concentration, c_{eq}, at equilibrium. The analysis provides the chemical or hydrophobic binding constant, K^0_D, of the detergent and the corresponding free energy. The free energies of binding, ΔG^0_{mem}, vary between −4 and −10 kcal/mol. They show a linear dependence on the chain length, which can be used to separate the contributions of the polar group and the hydrocarbon tail in membrane binding. The neutral maltose and the cationic $^{+}N(CH_3)_3$ headgroup show steric repulsion energies of about 2.5 kcal/mol counteracting the hydrophobic binding of the alkyl tail, whereas the anionic SO_4^- headgroup makes almost no contribution to membrane binding. The chemical nature of the headgroup influences the packing density of the hydrocarbon chains in the lipid bilayer with $^{+}N(CH_3)_3$ eliciting the weakest chain−chain interaction. The minimum repulsive interaction of the SO_4^- polar group makes the sodium *n*-alkyl-sulfates much stronger detergents than the nonionic or cationic counterparts, the binding constants, K^0_D, being 10−50 times larger than those of the corresponding *n*-alkyl-trimethylammonium chlorides. The membrane insertion was further compared with micelle formation of the same detergent. A cooperative aggregation model which includes all possible aggregation states is proposed to analyze micelle formation. The partition function can be defined in closed form, and it is straightforward to predict the thermodynamic properties of the micellar system. When aggregated in micelles, the detergent polar groups are in direct interaction and are not separated by lipid molecules. Under these conditions the SO_4^- group exhibits a strong electrostatic repulsive effect of 3.2 kcal/mol, while the contributions of the maltose and $^{+}N(CH_3)_3$ headgroups are very similar to those in the lipid bilayer.

Introduction

Membrane biology uses a wide variety of detergents to solubilize membranes and to purify lipids and membrane proteins. Most common are neutral detergents such as octyl glucoside or dodecyl maltoside, as they provide a nondenaturing environment. In contrast, charged detergents such as sodium dodecyl sulfate (SDS) not only dissolve membranes but simultaneously denature membrane-bound proteins, allowing molecular weight determinations by SDS gel chromatography. Positively charged detergents, on the other hand, have found widespread industrial applications. For example, dodecyltrimethylammonium chloride, $C_{12}H_{25}N(CH_3)_3^+Cl^-$ (DTAC), is used in commercial formulations for emulsifiers, textile fiber softeners, antistatic agents, or hair conditioners. Hazard identifications of DTAC are, among others, severe skin and eye burns, suggesting that DTAC can easily be absorbed by epithelial membranes. It is thus surpising that there is a dearth of quantitative information on the interaction of ionic detergents with lipid membranes. To the best of our knowledge, no systematic study comparing the membrane binding characteristics of cationic and anionic detergents is available. Thus, it is unknown to which extent the change from a nonionic to an ionic headgroup will change the binding properties, the bilayer stability, or the packing density of the hydrocarbon chains. As many biological membranes carry negatively charged lipids, the separation of electrostatic attraction or repulsion from hydrophobic binding is also a matter of concern. In the present study we have used high-sensitivity isothermal titration calorimetry (ITC) to measure the binding of *n*-alkyl-$^{+}N(CH_3)_3Cl^-$ and *n*-alkyl-$SO_4^-Na^+$ detergents to neutral and anionic lipid model membranes. The binding enthalpy and the binding isotherm were

* To whom correspondence should be addressed. Tel.: +41-61-267 2190. Fax: +41-61-267 2189. E-mail: joachim.seelig@unibas.ch.

10.1021/jp107088d
Published on Web 11/10/2010

the primary experimental result. The binding isotherm was interpreted in terms of a surface partition equilibrium, separating electrostatic effects from hydrophobic or chemical binding. The chain length of both types of detergents was varied systematically between 10 and 16 carbon atoms to elucidate the specific influence of the headgroups. The phase boundary between bilayer membranes and mixed micelles was deduced with dynamic light scattering (DLS) and correlated with the critical micelle concentration (cmc). Finally, a cooperative aggregation model was applied to describe the monomer−micelle equilibrium.

It was found that the change from an anionic to a cationic detergent headgroup has remarkable consequences for the membrane interaction. While SDS is leading readily to membrane micellization, the cationic counterpart DTAC forms stable bilayers even with large amounts of detergent in the membrane. The *n*-alkyl trimethylammonium salts can thus integrate easily into membranes and become true membrane constituents, while the *n*-alkyl sulfates destroy lipid bilayers. Both steric and electric repulsive interactions of the headgroups and the change in the packing density of the hydrocarbon tail must be considered for a quantitative interpretation.

Materials and Methods

Materials. 1-Palmitoyl-2-oleoyl-*sn*-glycero-3-phosphocholine (POPC) and 1-palmitoyl-2-oleoyl-*sn*-glycero-3-phosphoglycerol (POPG), dissolved in chloroform, were from Avanti Polar Lipids (Birmingham, AL). Decyltrimethylammonium chloride (DeTAC), dodecyltrimethylammonium chloride (DTAC), tetradecyltrimethylammonium chloride (TTAC), and hexadecyltrimethylammonium chloride were from Anatrace (Maumee, OH, USA). Sodium dodecyl sulfate, SDS, and sodium tetradecyl sulfate were from Sigma Aldrich (Steinheim, Germany).

Liposome Preparation. Composite lipid films were prepared by appropriate mixing of the lipids in chloroform. The solvent was removed under high vacuum. The dried lipid was suspended in buffer, vortexed, and freeze−thawed for five cycles. Unilamellar vesicles (LUVs) of diameter $d = 100$ nm were obtained by extrusion of multilamellar lipid suspensions through polycarbonate filters (Nuclepore, Pleasanton, CA).[1,2] Lipid concentrations were determined gravimetrically by carefully weighing the samples and by adding defined amounts of buffer. If not otherwise stated, the buffer composition was 25 mM 4-(2-hydroxyethyl)-1-piperazineethanesulfonic acid (HEPES; pH 7.5), 0.1 M NaCl. The phospholipid dispersions as well as the detergent solutions were prepared in the same buffer to minimize heats of dilution.

High-Sensitivity Titration Calorimetry. ITC was performed using a high-sensitivity titration calorimeter from MicroCal (Northampton, MA). To avoid air bubbles, solutions were degassed under vacuum before use. The calorimeter was calibrated electrically. The data were acquired by computer software developed by MicroCal. In control experiments the corresponding detergent solution (or vesicle suspension) was injected into buffer without lipid (or detergent). Injection of lipid suspensions into buffer alone yielded small reaction heats.

Light Scattering and Monolayer Measurements. Light scattering measurements were performed on a Zetasizer Nano-ZS instrument (ZEN3600; Malvern Inst., Worcestershire, UK). It was equipped with a 4 mW HeNe laser with a wavelength of 633 nm. Because of the principle of noninvasive back scattering, the scattering angle was 173°. The buffer was filtered through a 0.2 μm regenerated cellulose filter (Infochroma AG, Zug, CH) before use. The results were evaluated using DTS software provided by Malvern and are given as *z*-average size. The *z*-average size gives two values, a mean value for the size and a width parameter known as the polydispersity index (PDI). This mean size is an intensity mean.

Monolayer measurements were performed with a Teflon trough designed by Fromherz (Mayer Feintechnik, Göttingen, Germany) connected to a Wilhelmy balance.[3]

Experimental Results

Binding of Cationic and Anionic Detergents to Lipid Vesicles. Both hydrophobic and electrostatic forces contribute to the binding of detergents to lipid membranes. ITC in combination with suitable models allows a quantitative separation of the two energy contributions.[4] Unilamellar lipid vesicles of 100 nm diameter were prepared by several extrusions through 100 nm Millipore filters. The lipid composition was either 100% POPC or a POPC/POPG (75/25 mol/mol) mixture. Binding of DTAC and other cationic detergents to pure POPC vesicles creates a positive surface potential which makes further binding increasingly difficult. In contrast, anionic POPC/POPG vesicles show the opposite effect. In the initial phase, electrostatic attraction distinctly enhances binding until the membrane surface charge is compensated. Once the membrane charge has been neutralized, further DTAC addition leads to the same electrostatic repulsion as noted for POPC vesicles.

Binding isotherms were determined by lipid-into-detergent titration experiments.[5] For the example given in Figure 1, the calorimeter cell contained DTAC at a total concentration of $c_D^0 = 80$ μM in buffer. Lipid vesicles composed of POPC/POPG (75/25 mol/mol) and $c_L^0 = 26.4$ mM were injected in 10 μL steps at 35 °C. Figure 1a displays the heat flow as a function of time. Each injection gives rise to an exothermic heat peak, h_i, produced by the insertion of the detergent into the membrane. h_i decreases with consecutive injections as the amount of free detergent in the calorimeter cell is reduced. The small heat peaks at the very end of the titration arise from dilution effects and are subtracted. In the following δh_i denotes the corrected heat of reaction. Figure 1b shows the corrected heats of reaction, δh_i, as a function of the injection number, n_i. The cumulative heat of reaction after k injections is $\sum_1^k \delta h_i$. The concentration of membrane-bound detergent, c_b, after k injections is then given by:

$$c_b^{(k)} = (\sum_1^k \delta h_i / \sum_1^m \delta h_i) c_D^0$$

where the subscript D stands for detergent and m is the number of injections until all of the detergent is bound. The free (equilibrium) detergent concentration in the calorimeter cell after k injections can be calculated according to

$$c_{eq}^{(k)} = c_D^0 - c_b^{(k)}$$

After k injections the concentration of lipid in the cell is

$$c_L^{(k)} = k V_{inj} c_L^0 / V_{cell}$$

where c_L^0 is the lipid concentration of the stock solution, V_{inj} is the injected volume per injection step, and V_{cell} is the volume of the calorimeter cell. The extent of detergent binding, X_b, is then defined as

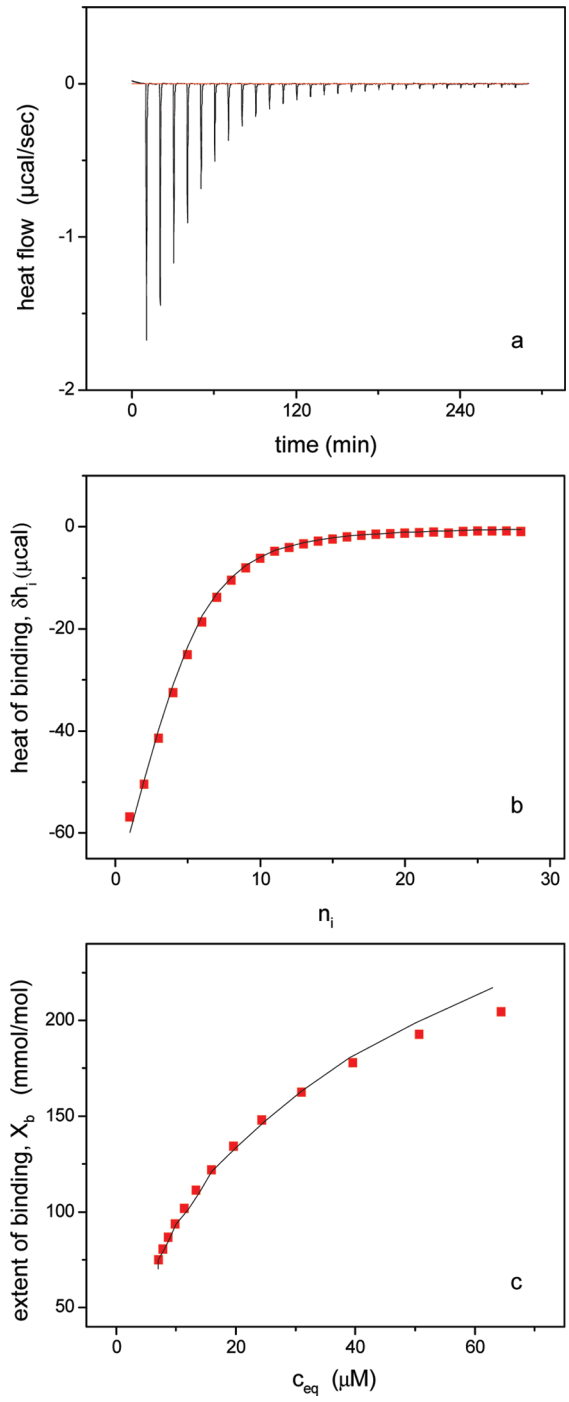

Figure 1. Partition equilibrium of DTAC with POPC/POPG (75/25 mol/mol) 100 nm lipid vesicles. (a) Lipid-into-DTAC titration. Titration calorimetry of DTAC (c_D^0 = 80 μM) with lipid vesicles (c_L^0 = 26.4 mM) in buffer (0.1 M NaCl, 25 mM HEPES, pH 7.5) at 35 °C. Each peak results from the addition of 10 μL vesicle suspension to the DTAC solution in the calorimeter cell (cell volume = 1.414 mL). (b) The reaction heats, δh_i, shown as a function of the injection number n_i. Experimental results (■) are compared with the theoretical analysis (solid line). (c) Binding isotherm for DTAC partitioning into the outer monolayer of POPC/POPG vesicles. The extent of binding, X_b, is defined as the molar ratio of bound DTAC, n_b, to total lipid, n_L^0, in the outer monolayer. ■, experimental results; solid line, theoretical prediction. The theoretical analysis in b and c is based on a partition constant of $K_D^0 = 3 \times 10^3$ M^{-1} and $\Delta H_{mem}^0 = -2.65$ kcal/mol. DTAC binding was assumed to follow a surface partition model according to $X_b = K_D^0 c_M$ where c_M is the surface concentration of detergent. It is related to the DTAC equilibrium concentration, c_{eq}, according to $c_M = c_{eq} \exp(-z\psi_0 F_0/RT)$.

$$X_b^{(k)} = \frac{c_b^{(k)}}{c_L^{(k)}}$$

It is thus possible to construct the binding isotherm $X_b = f(c_f)$ in a model-independent manner as shown in Figure 1c.

The next step is the interpretation of the experimental binding isotherms in terms of a physically realistic model. The approach chosen here is the electrostatic attraction/repulsion of detergent to the membrane surface followed by a partitioning into the membrane (to be discussed in more detail below). Anticipating the results of this analysis, the solid lines in Figure 1b,c were calculated with the binding constant, K_D^0, and the heat of membrane binding, ΔH_{mem}^0, listed in Table 1. Because of its charged headgroup, DTAC cannot easily flip to the inner membrane. In fact, DTAC concentrations ~80−100 times higher than those used in the ITC experiments are needed to induce membrane dissolution (cf. Figure 3). The analysis of the ITC binding isotherms was therefore based on a half-sided binding of DTAC to the outer monolayer only. Consistent results over the whole temperature range of 15−65 °C were obtained.

Figure 2a shows the temperature dependence of the DTAC binding enthalpy, ΔH_{mem}^0, for both neutral and anionic vesicles. The regression analysis of the data in Figure 2a (solid lines) provides the molar heat capacity change with $\Delta C_p^0 = -68$ cal/mol K (−80 cal/mol K) for POPC (POPC/POPG 75/25 mol/mol) 100 nm vesicles. As the binding enthalpy, ΔH_{mem}^0, is negative at all temperatures, the binding constant, K_D^0, will decrease at higher temperatures as evidenced experimentally by Figure 2b. The solid lines are the predicted temperature dependencies for the two membranes using van't Hoff's law and the temperature-dependent ΔH_{mem}^0-values listed in Table 1.

For micelles it is often assumed that the polar group and the alkyl chain make independent contributions to the free energy.[6] In a single ITC experiment, however, only the sum of the free energies of head and tail is measured. To separate these energies, we have varied the length of the hydrocarbon chain from 10 to 16 C-atoms for the $^+N(CH_3)_3$ polar group. The corresponding experimental results are summarized in Table 2. At 25 °C the reaction enthalpies, ΔH_{mem}^0, are rather small and exothermic and show no systematic variation with the chain length. In contrast, the binding constant K_D^0 increases systematically by a factor of 10−20 upon each addition of a two-carbon segment. The corresponding change in free energy is about −1 to −1.5 kcal/mol. If the positively charged $^+N(CH_3)_3$ group is replaced by the negatively charged SO_4^- group, the K_D^0 values are 10−50 times larger. This suggests different types of interactions for the SO_4^- and $^+N(CH_3)_3$ headgroups upon membrane binding which will be discussed below. For comparison, Table 2 also contains data for the nonionic detergent *n*-alkyl-maltoside.[5] The reaction enthalpies are endothermic, but the binding constants are rather similar to those of *n*-alkyl-$^+N(CH_3)_3$.

Membrane Solubilization. At sufficiently high detergent concentrations lipid bilayers become destabilized, leading to mixed micelles composed of lipid and detergent. We denote with $X_b^{sat} = c_b^{sat}/c_L^0$ the beginning of this process, that is, the phase boundary between the pure bilayer phase and the coexistence phase of bilayers with mixed micelles. c_b^{sat} is the concentration of the membrane-bound detergent at the point where no further detergent uptake is possible. Likewise, $X_b^{sol} = c_b^{sol}/c_L^0$ denotes the detergent/lipid molar ratio at the end of the solubilization process and describes the phase boundary between the coexistence phase and the pure micellar phase.

When measuring the phase boundaries, it must be noted that DTAC cannot easily translocate across the bilayer membrane

TABLE 1: POPC or POPC/POPG (75/25 mol/mol; 100 nm) Vesicles Titrated into DTAC Solution[a]

temp. (°C)	c_D^0 (μM)	c_L^0 (mM)	POPC/POPG (%)	K_D^0 (M^{-1})	ΔH_{mem}^0 (kcal/mol)	ΔG_{mem}^0 (kcal/mol)	$T\Delta S_{mem}^0$ (kcal/mol)
25	40	23.86	100/0	3.5×10^3	−0.99	−7.18	6.19
35	20	26.5	100/0	3.3×10^3	−1.48	−7.39	5.91
35	40	26.5	100/0	3.3×10^3	−1.43	−7.39	5.96
45	30	25.19	100/0	3.0×10^3	−2.35	−7.57	5.22
25	50	24.55	75/25	3.6×10^3	−0.96	−7.20	6.24
35	80	26.04	75/25	3.1×10^3	−2.23	−7.35	5.12
45	80	26.26	75/25	2.8×10^3	−2.87	−7.53	4.66
55	80	26.87	75/25	2.4×10^3	−3.53	−7.66	4.13
55	80	26.87	75/25	2.4×10^3	−3.87	−7.66	3.79
55	80	26.21	75/25	2.2×10^3	−3.61	−7.61	4.00
65	80	26.47	75/25	2.1×10^3	−4.21	−7.81	3.60
35	80	26.03	75/25	3.3×10^3	−2.08	−7.39	5.31
45	80	26.3	75/25	3.0×10^3	−3.86	−7.57	3.71
55	80	26.06	75/25	2.4×10^3	−3.94	−7.66	3.72

[a] Measurements in buffer (0.1 M NaCl, 25 mM HEPES, pH 7.5).

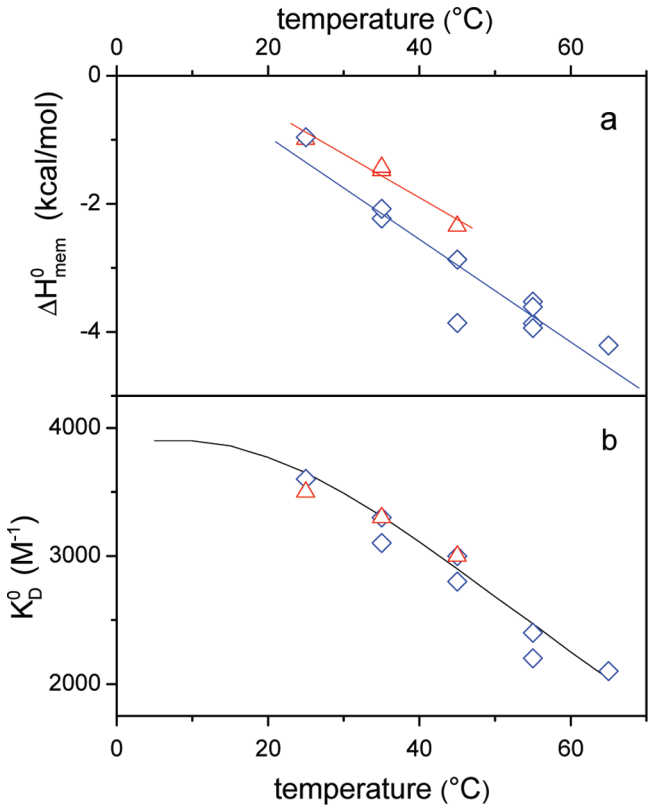

Figure 2. Thermodynamic parameters of DTAC partitioning into POPC and POPC/POPG (75/25 mol/mol) 100 nm vesicles. (a) Temperature dependence of the membrane binding enthalpy ΔH_{mem}^0. △, POPC vesicles; ◇, mixed POPC/POPG vesicles. (b) Temperature dependence of the binding constant K_D^0. The solid line is the theoretical prediction calculated with the van't Hoff equation and the temperature-dependent ΔH_{mem}^0 values for POPC/POPG vesicles shown in a.

because of its electric charge. This leads to a kinetic hindrance of the solubilization process as illustrated by Figure 3. POPC/POPG (75/25 mol/mol) vesicles of 100 nm diameter and at a lipid concentration of $c_L^0 = 100$ μM were suspended in $c_D^0 =$ 80.4 mM DTAC (∼10 × cmc), and the change in absorbance was measured in a UV spectrometer at 350 nm as a function of time and temperature. Figure 3 demonstrates that membrane solubilization is a slow process, even at high detergent concentrations, with a half-time of about 50 min at room temperature, decreasing to a few minutes as the temperature is increased to 45 °C.

Long equilibration times of ∼12 h were hence employed to deduce the phase diagram between bilayers and micelles at 25 °C. Lipid vesicles and DTAC were mixed together at defined ratios, and the size of the mixed lipid/DTAC vesicles was measured with DLS 12 h later. Figure 4a summarizes the DLS measurements at 25 °C. The vesicle size at a defined lipid concentration is plotted versus the total detergent concentration. Each data point in Figure 4a corresponds to a separate lipid vesicle/detergent preparation. The initial vesicle size (at low DTAC concentration) is 90−120 nm and is characterized by a monomodal size distribution (polydispersity index <0.2). The vesicle size decreases rapidly after the point of membrane saturation, X_b^{sat}, is reached (PDI up to 0.7). As the total detergent concentration, c_D^0, is the sum of the DTAC equilibrium concentration at saturation, c_{eq}^{sat}, and bound detergent $c_b^{sat} = X_b^{sat} c_L^0$, it follows:[7]

$$c_D^0 = c_{eq}^{sat} + X_b^{sat} c_L^0$$

A plot of the total detergent concentration, c_D^0, at saturation versus the total lipid concentration, c_L^0, should yield a straight line with a slope of X_b^{sat} and an intercept c_{eq}^{sat}. This is borne out experimentally in Figure 4b where c_D^0 is plotted versus c_L^0 for the saturation limit. Regression analysis of the data in Figure 4b yields for the saturation limit

$$c_D^0 = 6.55 + 1.29 c_L^0 \qquad (R = 0.98)$$

The minimum bound detergent-to-lipid ratio at which micelle formation sets in is $X_b^{sat} = 1.29 \pm 0.11$ mol DTAC bound/mol lipid. The minimum concentration of DTAC to initiate bilayer disruption at 25 °C is $c_{eq}^{sat} = 6.55 \pm 0.22$ mM, which is clearly below the cmc of ∼10 mM at this temperature.

The phase boundary for *complete* solubilization, characterized by X_b^{sol}, can also be deduced from Figure 4a. Using DLS we determine the total DTAC concentration, c_D^0, where for a given lipid concentration, c_L^0, the absorption reaches its minimum (polydispersity index <0.25). A plot according to the above equation is shown in 4b and yields

$$c_D^0 = 6.85 + 1.96 c_L^0 \qquad (R = 0.99)$$

The bound detergent-to-lipid ratio at complete solubilization is thus estimated as $X_b^{sol} \approx 1.96 \pm 0.1$ mol DTAC bound/mol lipid. The limiting concentration is $c_{eq}^{sol} = 6.85 \pm 0.2$ mM. For membrane solubilization purposes DTAC must be considered a "weak" detergent.[5]

TABLE 2: Comparison of Detergents as a Function of Chain Length[a]

micelle formation							membrane partitioning					
headgroup	n	cmc (mM)	ΔG^0_{mic}[b] (kcal/mol)	ΔH^0_{mic} (kcal/mol)	$T\Delta S^0_{mic}$ (kcal/mol)	reference	membrane composition	K^0_D (M^{-1})	ΔG^0_{mem}[c] (kcal/mol)	ΔH^0_{mem} (kcal/mol)	$T\Delta S^0_{mem}$ (kcal/mol)	reference
maltose	8	19.5	−4.69	2.39	7.08	27	POPC[d]	25	−4.27	2.4	6.67	5
	10	1.8	−6.10	3.35	9.45	27	POPC	200	−5.50	3.1	8.60	5
	12	0.17	−7.49	0.96	8.45	27	POPC	5000	−7.40	1.0	8.40	5
$^+N(CH_3)_3$	10	74.1	−3.91	1.57	5.48	this work	POPC/POPG[e] 3:1	355	−5.83	−0.38	5.45	this work
	12	9.01	−5.15	0.80	5.95	this work	POPC/POPG 3:1	3600	−7.20	−0.96	6.24	this work
	14	0.77	−6.60			8	POPC/POPG 3:1	1.60×10^4	−8.08	−2.51	5.57	this work
$^+N(CH_3)_3$	12						POPC	3.50×10^3	−7.18	−0.99	6.19	this work
	12						POPC[f]	5.2×10^3	−7.72	−2.1	5.62	this work
	14						POPC[f]	6.0×10^4	−9.22	−1.5	7.72	this work
	16						POPC[f]	3.5×10^5	−10.3	−1.0	9.3	this work
$-SO_4^-$	10	13.3	−4.92	−0.29		this work	POPC	2.73×10^3	−7.04	−3.84	3.20	this work
	12	1.57	−6.18	−0.80	5.38	11, 28	POPC	3.30×10^4	−8.51	−4.23	4.28	this work
	14	0.2	−7.40			29	POPC	5.00×10^5	−10.11	−2.69	7.42	this work
$-SO_4^-$	10						POPC/POPG 3:1	7.00×10^3	−7.59	−1.33	6.27	this work
	12						POPC/POPG 3:1	3.70×10^4	−8.58	−3.7	4.88	this work
	14						POPC/POPG 3:1	6.50×10^5	−9.66	−2.42	7.23	this work

[a] 25 °C, 0.1 M NaCl, with or without 25 mM HEPES buffer pH 7.5. [b] Calculated according to $\Delta G^0_{mic} = RT \ln(cmc/55.5)$. [c] Calculated according to $\Delta G^0_{mem} = -RT \ln(55.5K^0_D)$. [d] POPC: 1-palmitoyl-2-oleoyl-*sn*-glycero-3-phosphocholine. [e] POPG: 1-palmitoyl-2-oleoyl-*sn*-glycero-3-phosphoglycerol. [f] 30 nm vesicles, 50 mM Tris, 0.114 M NaCl, 37 °C, pH 7.4.

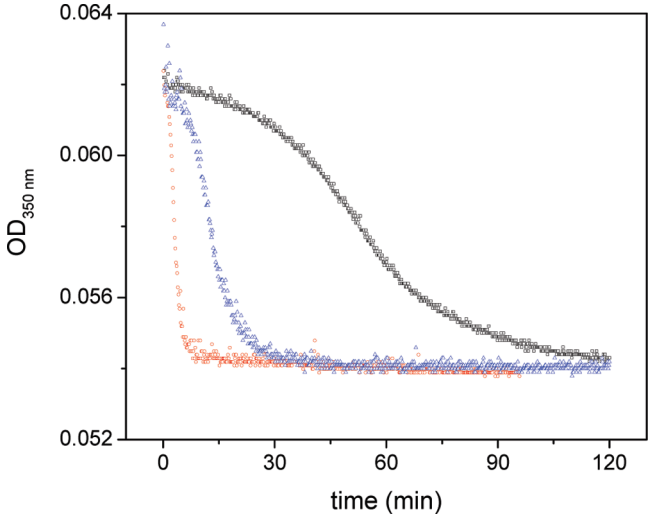

Figure 3. Kinetics of vesicle dissolution by DTAC. POPC/POPG vesicles ($c^0_L = 100$ μM) were mixed with 80.4 mM DTAC, and the optical density was monitored as a function of time and temperature. The temperatures are from right to left: 25, 35, and 45 °C.

Critical Micellar Concentration (cmc) Measured by ITC. To compare membrane insertion with micelle formation, it was necessary to measure the cmc under exactly the same conditions as used for membrane insertion. ITC is a convenient method to determine the cmc of a detergent. A concentrated detergent solution with $c \gg$ cmc is injected in small steps into buffer, and the heat of demicellization, δh_i, is recorded. Under ideal conditions δh_i should be constant during the first few injections until the concentration of detergent in the calorimeter cell approaches the cmc. Near the cmc the heat flow decreases rapidly as the injected micelles no longer disintegrate. Figure 5 shows a typical titration diagram and its evaluation by a model discussed below. Figure 5a displays the heat flow measured for 10 μL injections of a buffered micellar solution of 100 mM DTAC into buffer (0.1 M NaCl, 25 mM HEPES, pH 7.5) at 65 °C. Figure 5b shows the integrated heat flows, δh_i, as a function of the injection number, n_i. The solid line is the theoretical prediction based on the aggregation model discussed below.

Figure 5c describes the degree of dissociation, α, equivalent to the mole fraction of detergent monomers. During the first few injections the injected micelles completely disintegrate into monomers (degree of dissociation α = 1). Under ideal conditions already the very first injection, δh_1, would be sufficient to calculate the heat of demicellization. As the injection continues, the detergent concentration in the calorimeter cell rises, and the degree of dissociation, α, starts to decrease as the micelles only partially disintegrate. The degree of dissociation can be calculated as a function of the injection number k:

$$\alpha_k = \frac{\sum_{i=1}^{k} \delta h_i}{k\delta h_1}$$

The measured heat, $\sum_{i=1}^{k}\delta h_i$, is divided by the maximum heat possible, $k\delta h_1$, expected for full dissociation. The experimental results are given by the solid symbols in Figure 5c.

Table 3 summarizes the thermodynamic parameters of micellization. It includes the variation of the enthalpy of micelle *formation*, $\Delta H^0_{mic} = -\Delta H^0_{demic}$, with temperature. Endothermic heats of micelle formation are observed at low temperatures, exothermic values above 35 °C. Linear regression analysis yields ΔH^0_{mic}(kcal/mol) = −0.095 T (°C) + 3.16. The molar heat capacity change is $\Delta C^0_p = -95$ cal/mol K. Previous cmc measurements obtained under slightly different conditions and evaluated by the mass action model are in broad agreement with the present results.[8]

Discussion

Surface Partition Model Describing Detergent−Membrane Interactions. The calorimetric titration experiment provides the extent of binding, X_b, as a function of the detergent equilibrium concentration, c_{eq}. No specific model is needed to deduce the binding isotherm $X_b = f(c_{eq})$. The next step is the interpretation of the binding isotherm in terms of a physically realistic model combining electrostatic attraction or repulsion to the membrane surface with hydrophobic or chemical sorption into the lipid bilayer. This is possible by introducing the surface concentration, c_M, which is the concentration of free detergent immediately above the plane of binding. For nonionic detergents c_M is identical to the equilibrium concentration, c_{eq}. For cationic detergents in contact with anionic lipid vesicles, electrostatic attraction yields $c_M > c_{eq}$. In contrast, insertion of cationic detergents into a neutral lipid bilayer leads to a positively

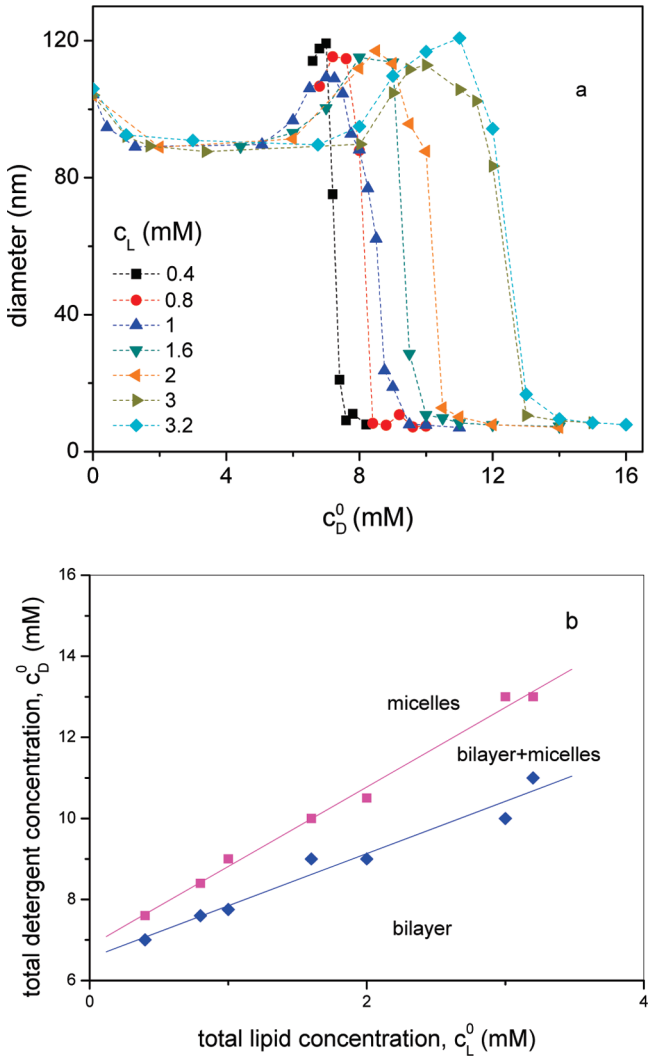

Figure 4. Saturation and solubilization of POPC/POPG 100 nm vesicles by DTAC. (a) Determination of vesicle size by DLS. Measurements in buffer (0.1 M NaCl, 25 mM HEPES, pH 7.5). Lipid and DTAC were mixed in defined concentrations. The mixture was equilibrated at 25 °C for 12 h. The average size of the resulting vesicles was then determined by DLS. Each data point in the figure corresponds to a separate lipid/DTAC preparation. The PDI before saturation was less than 0.2; after solubilization the PDI was <0.25. c_D^0 is the total monomer concentration of detergent. (b) Phase diagram. The total detergent concentration at saturation or solubilization is plotted against the corresponding total lipid concentration. ♦, saturation boundary; ■, solubilization boundary.

charged membrane surface, making insertion increasingly difficult and leading to $c_M < c_{eq}$.

The surface concentration, c_M, is related to the surface potential, ψ_0, of the lipid membrane and the detergent equilibrium concentration, c_{eq}, according to Boltzmann's law

$$c_M = c_{eq} \exp(-zF_0\psi_0/RT)$$

(z = signed valence of detergent, F_0 = Faraday constant). ψ_0, in turn, depends on the charge density of the membrane, the extent of detergent binding, the ionic strength of the buffer solution, and so forth, and can be calculated with the Gouy−Chapman theory.[9,10] It is then possible to correlate the measured X_b-values with c_M in terms of a *surface partition* equilibrium

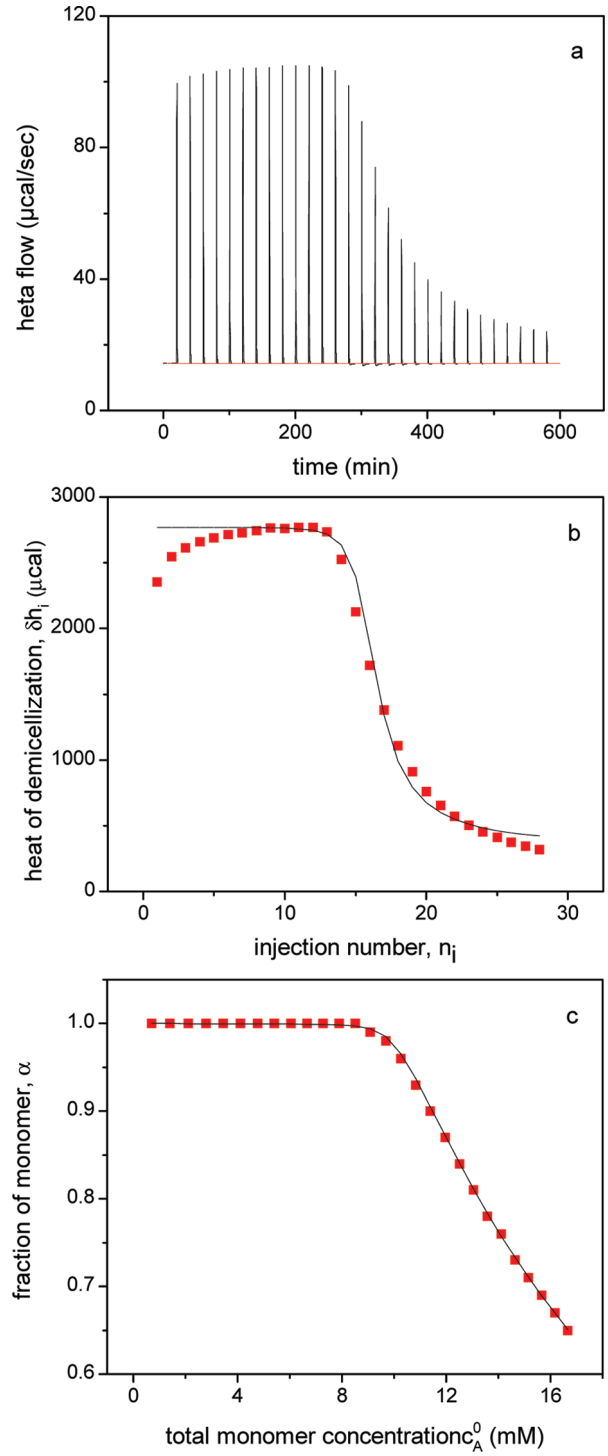

Figure 5. Demicellization reaction of DTAC. (a) Titration calorimetry of DTAC (c_D^0 = 100 mM) in buffer (0.1 M NaCl, 25 mM HEPES, pH 7.5) into pure buffer of the same composition (at 65 °C). Each peak corresponds to the injection of 10 μL of DTAC solution into the calorimeter cell (cell volume 1.414 mL). (b) Heat of demicellization, δh_i, as a function of injection number. Neglecting additional dilution effects, the heat of micelle disintegration is constant for the first 12 injections but decreases rapidly as the detergent concentration in the calorimeter cell approaches the cmc. The solid line is the theoretical prediction calculated with the aggregation model described in the text. The corresponding parameters are $K_D^0 = 97\ M^{-1}$ (cmc = $1/K_D^0 = 10.31$ mM), $\Delta H_D^0 = -2770$ cal/mol, $\sigma = 10^{-4}$, $n = 45$. (c) The fraction of monomers, $\alpha = c_A/c_A^0$, as a function of the total detergent concentration in the calorimeter cell. During the initial injections, the ~100 fold dilution leads to a complete dissolution of micelles and $\alpha = 1$. The solid line is again the theoretical analysis calculated with the same parameters as above.

TABLE 3: Thermodynamic Parameters of Micelle Formation of DTAC and DeTAC[a]

	temp (°C)	K^0_{mic} (M^{-1})	cmc (mM)	ΔH^0_{mic} (kcal/mol)	ΔC^0_p (cal/mol K)	micelle size n	cooperativity σ
DTAC (C12)	15	103	9.71	1.92		60	10^{-4}
	25	111	9.01	0.80		60	10^{-4}
	35	113	8.85	−0.28	−94.6	45	10^{-4}
	45	116	8.62	−1.33		45	10^{-4}
	45	110	9.09	−1.27		45	10^{-4}
	65	97	10.31	−2.77		45	10^{-4}
DeTAC (C10)	25	13.5	74.1	1.57		40	10^{-4}

[a] Measurements in buffer (0.1 M NaCl, 25 mM HEPES, pH 7.5).

$$X_b = K^0_D c_M$$

The details of this approach have been described in previous publications.[4,5,11] The partition or binding constant, K^0_D, refers to the chemical or hydrophobic affinity after eliminating electrostatic attraction or repulsion effects. The free energy of the hydrophobic membrane binding step can then be calculated as

$$\Delta G^0_{mem} = -RT \ln c_w K^0_D$$

where $c_w = 55.5$ is the molar concentration of water and corrects for the cratic contribution.[12]

Table 2 summarizes the binding constants, K^0_D, and the corresponding free energies, ΔG^0_{mem}, for the different detergents and membranes investigated. It should be obvious that the experimental binding isotherms are quite different if the bilayer is electrically neutral as for 100% POPC or charged as for POPC/POPG (75/25 mol/mol). Inspection of Table 2 then shows that the Gouy−Chapman analysis yields hydrophobic binding or partition constants which are almost identical for the two types of membranes. After correcting for electrostatic effects, the remaining hydrophobic interaction energy of a given detergent is independent of the chemical nature of the lipids. To be more specific: the binding constants, K^0_D, of DTAC to 100 nm POPC and mixed POPC/POPG (75/25 mol/mol) vesicles are 3500 M^{-1} and 3600 M^{-1}, respectively (at 25 °C). At a DTAC concentration of $c_{eq} = 65\ \mu M$ the extent of DTAC binding to neutral POPC vesicles is only $X_b = 0.09$ mol/mol, leading to a repulsive potential of $\psi_0 = +24$ mV and a surface concentration of $c_M = 25.8\ \mu M$. In contrast, anionic POPC/POPG (75/25 mol/mol) membranes equilibrated at the same concentration bind distinctly more DTAC with $X_b = 0.234$ mol/mol which together with the bound Na^+ to POPG ($X_{Na^+} = 0.016$ mol/mol) exactly compensates the membrane surface charge. Under these conditions the surface potential is zero, and the surface concentration c_M equals the equilibrium concentration c_{eq} ($c_M = c_{eq} = 65\ \mu M$).

Separating Polar and Nonpolar Interactions for Membrane Binding. The dominant driving force for detergent insertion comes from the hydrocarbon chains via the hydrophobic effect, whereas the contribution of the polar groups is less clear. To quantitate the influence of the headgroups let us first compare the membrane binding of three detergents with the same C-12 alkyl chain, that is, dodecylmaltoside (DDM), DTAC, and SDS, which have binding constants of $K^0_D = 5 \times 10^3\ M^{-1}$, $3.5 \times 10^3\ M^{-1}$, and $3.3 \times 10^4\ M^{-1}$, respectively, for POPC vesicles at 25 °C. The question arises if the observed differences in K^0_D can be assigned exclusively to the different headgroups or if the ordering of the hydrocarbon chains is also affected. To this purpose, Figure 6a shows the free energy, ΔG^0_{mem}, plotted against the length of the hydrocarbon chain. The slopes of the straight lines measured for neutral POPC bilayers

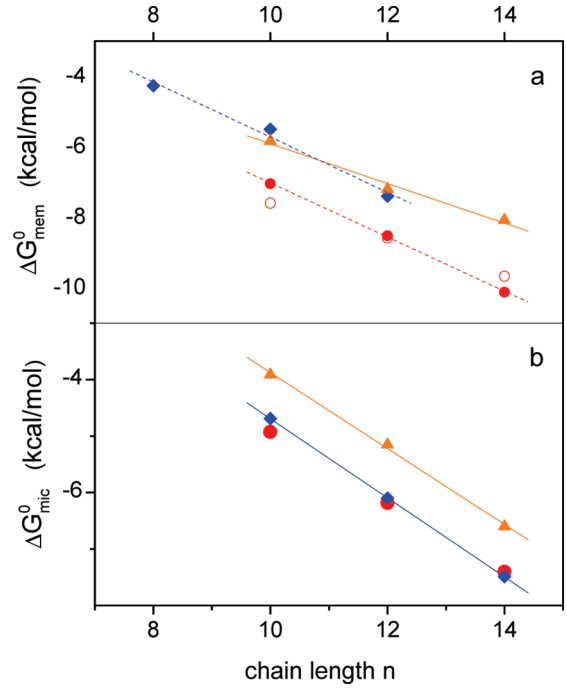

Figure 6. Membrane partitioning and micelle formation as a function of the length of the alkyl chain. Comparison of neutral, anionic, and cationic detergents. (a) Free energy, ΔG^0_{mem}, of membrane partitioning (corrected for electrostatic effects). ◆, *n*-alkyl maltose and POPC bilayers; ▲, *n*-alkyl-$^+N(CH_3)_3$ and POPC/POPG (75/25 mol/mol) bilayers; ●, *n*-alkyl-SO_4^- and POPC; ○, *n*-alkyl-SO_4^- and POPC/POPG (75/25 mol/mol). (b) Free energy of micellization ΔG^0_{mic}. Headgroup symbols as above.

are −782 cal/mol for *n*-alkyl-maltoside, −769 cal/mol for *n*-alkyl-SO_4^-, and −646 cal/mol for *n*-alkyl-$^+N(CH_3)_3$. These numbers denote the free energy contribution of a single $-CH_2-$ segment (ΔG_{CH_2}) to membrane binding. The figure demonstrates that the head and tail are not completely decoupled in their energy contributions but that the chemical nature of the headgroup influences the packing of the tail. This is in contrast to the assumption stated above for micelles.[6] Knowledge of ΔG_{CH_2} makes it possible to estimate more precisely the contribution of the headgroups to the binding process. Following a proposal of Tanford for micelles[6] (p 72), the contribution of the alkyl chain is estimated as $\Delta G_{chain} = -2100 + (n_c - 2) \times \Delta G_{CH_2}$. The first term on the right side denotes the contribution of the terminal methyl group, while n_c is the total number of carbon atoms of the alkyl chain. Two carbon atoms are not counted because one is the CH_3 group and the other is the $-CH_2-$group next to the polar group. Subtracting ΔG_{chain} from the total free energy of insertion, ΔG^0_{mem}, yields the free energies of the polar groups as 2.5 kcal/mol for maltose, 2.6 kcal/mol for $^+N(CH_3)_3$, and 0.1 kcal/mol for SO_4^-.

The surface area requirements of the $^+N(CH_3)_3-$ and the maltose headgroup were determined in monolayer experiments

by measuring the Gibbs adsorption isotherm and were $A_D = 54 \pm 5$ Å^2 and 64 ± 4 Å^2, respectively. The insertion of a molecule of area A_D into the bilayer surface requires work against the lateral packing pressure π, and the corresponding energy is πA_D.[3,13,14] For POPC bilayers at 25 °C the lateral packing pressure was determined as $\pi = 32$ mN/m.[15] This leads to insertion energies of 2.5 kcal/mol for $^{+}N(CH_3)_3$ and 2.9 kcal/mol for maltose in good agreement with the above extrapolations. No monolayer measurements were made for the SO_4^- group. On the basis of comparisons of molecular models, the surface area requirement of the SO_4^- group is about 1/5 of that of the $^{+}N(CH_3)_3$ group. This predicts a headgroup insertion energy of at most 0.5 kcal/mol, again consistent with the observation described above.

The analogous analysis for the headgroup contribution was carried out for micelle formation. Figure 6b shows the free energy of micelle formation, $\Delta G^0_{mic} = RT \ln(\text{cmc}/55.5)$, plotted against the length of the alkyl chain. Almost parallel lines are obtained with slopes of $\Delta G_{CH_2} = -700$ cal/mol for *n*-alkyl-maltoside, -620 cal/mol for *n*-alkyl-SO_4^-, and -620 cal/mol for *n*-alkyl-$^{+}N(CH_3)_3$, as observed before the chemical nature of the headgroup influences the packing of the hydrocarbon chains. The contribution of the headgroups to micelle formation can again be calculated by subtracting the alkyl chain contribution from the total free energy of micelle formation yielding 1.7 kcal/mol for maltose headgroup, 2.3 kcal/mol for $^{+}N(CH_3)_3$, and 3.2 kcal/mol for SO_4^-. For maltose and $^{+}N(CH_3)_3$ the repulsive energy contributions in micelles are similar to those in membranes, which is understandable if the interaction is based on steric repulsion. For the SO_4^- polar group the repulsive energy increases dramatically in the micelle, suggesting that electrostatic repulsion dominates in the micelle but is diluted out in the POPC membrane.

The free energy change by removing a $-CH_2$-group from water and inserting it into bulk liquid carbon is about -820 cal/mol.[6] The ΔG_{CH_2} for membrane insertion is lower with -775 ± 10 cal/mol for *n*-alkyl-maltoside and $-SO_4^-$ and -650 cal/mol for *n*-alkyl-$^{+}N(CH_3)_3$. Micelle formation leads to even smaller ΔG_{CH_2} values if membrane and micelle are compared for the same detergent. In the case of micelles it has been argued that the difference between bulk hydrocarbon and micelle can be explained by the more restricted motion in the micelle.[6] However, the chain motion is even more restricted in the lipid membrane, but ΔG_{CH_2} is closer to liquid hydrocarbons. Alternatively, it could be reasoned that the accessibility of the *n*-alkyl chains to water is different in the three environments and increases in the order bulk hydrocarbon < membrane < micelle. ΔG_{CH_2} becomes less negative in the same order and may thus reflect a decrease in the hydrophobic effect.

The linearity of ΔG^0_{mem} with the length of the detergent chain is quite surprising. We have recently studied the influence of a nonionic detergent, *n*-alkyl-β-D-glucopyranoside (β-OG), on the order profile of a bilayer composed of phospholipids with two C-18 chains (POPC).[16] POPC was selectively deuterated at various segments of the palmitic acyl chain, and the segmental fluctuations were measured with deuterium NMR and quantitated in terms of the order parameter. The experiments showed that β-OG with short alkyl chains ($n = 6$ or 7) led to a large disturbance of the order profile, whereas the effect of β-OGs with $n = 10$ was more modest but still significant. The data prove that the lipid bilayer changes its structure upon insertion of detergent, and the change in free energy, ΔG_{CH_2}, is thus the combined effect of the detergent−lipid interaction and a bilayer restructuring. We are at present performing analogue ^{2}H NMR experiments with the two types of ionic detergents discussed in this work.

Phase Diagram for Membrane Solubilization. Micelle formation and membrane insertion are energetically similar processes. The free energy of micelle formation is $\Delta G^0_{mic} = RT \ln \text{cmc}/c_w$ and that of membrane insertion $\Delta G^0_{mem} = -RT \ln c_w K^0_D$. The energy difference $\delta\Delta G = RT \ln \text{cmc} \times K^0_D$ determines which process is favored. For cmc $\times$ $K^0_D \gg 1$ membrane insertion is preferred, while micelle formation occurs at cmc $\times$ $K^0_D \ll 1$. We have shown for a series of nonionic detergents that an approximately linear relationship exists between the free energies of micellization and membrane insertion.[5,17] This concept was extended to calculate the limiting bound detergent-to-lipid ratio, X^{sat}_b, which initiates membrane destabilization. For nonionic detergents X^{sat}_b could be approximated by the following relationship[18]

$$X^{sat}_b = K \times \text{cmc}$$

DDM has a cmc = 0.17 mM and a $K^0_D = 5000$ M^{-1} for POPC bilayers leading to a calculated $X^{sat}_b = 0.85$ mol/mol, in good agreement with the experimental value of $X^{sat}_b \approx 0.9$.[19] The above equation must be modified however for ionic detergents as the detergent concentration near the membrane surface is not the cmc but the surface concentration $c_M = \text{cmc} \times \exp(-zF_0\psi_0/RT)$. Considering DTAC, the detergent mainly discussed in this work, the cmc is 9.01 mM, and the binding constant is $K^0_D = 3500$ M^{-1} for POPC/POPG (75/25 mol/mol) bilayers (in buffer; 25 °C). The surface concentration of detergent can be calculated as $c_M = 0.33$ mM, leading to $X^{sat}_b = 1.17$ mol/mol which may be compared with the experimental value of $X^{sat}_b = 1.29$. It should be realized that at $X_b = 0.25$ the negative charge of the POPC/POPG (75/25) membrane is exactly compensated by the cationic detergent. X_b values > 0.25 lead to positively charged membranes and the surface concentration c_M of detergent will become distinctly smaller than the bulk concentration.

The 10−20 fold higher membrane binding constants of the *n*-alkyl-sulfates explain why lower equilibrium detergent concentrations are needed to induce membrane disruption compared to the nonionic or cationic detergents investigated here. By adding SDS and DTAC to headgroup-deuterated POPC and measuring the ^{2}H and ^{31}P NMR spectra, we observed that DTAC moves the choline moiety toward the water phase while SDS induces the opposite movement, rotating the $^{-}$P-$^{+}$N dipole deeper into the plane of the membrane. These structural changes agree with the "molecular voltmeter concept" described earlier.[20] The different orientations of the phosphocholine headgroups must entail changes in the lipid−lipid interaction energies. A quantitative analysis of the NMR data will be published separately.

Cooperative Aggregation as a Model for Micelle Formation. In the literature ITC demicellization data are usually evaluated by either the pseudophase separation model or by a mass action equilibrium. Both models describe an all-or-none process and neglect species with intermediate aggregation numbers. As a new model we propose a cooperative aggregation model for micelle formation. This model has been employed successfully in other aggregation processes of biomolecules.[12,21,22] It starts with a *nucleation step*

$$A + A \overset{\sigma K}{\rightleftharpoons} A_2 \qquad c_{A_2} = \sigma K c_A{}^2$$

followed by n growth steps.

$$A_2 + A \overset{K}{\rightleftharpoons} A_3 \qquad c_{A_3} = Kc_{A_2}c_A = \sigma K^2 {c_A}^3$$

$$\vdots$$

$$A_{n-1} + A \overset{K}{\rightleftharpoons} A_n \qquad c_{A_n} = Kc_{A_{n-1}}c_A = \sigma K^{n-1} {c_A}^n$$

K is the equilibrium constant of the growth step, while σ is the nucleation parameter inducing cooperativity. σ is much smaller than 1 as the initial dimer formation (nucleation) is more difficult than the additional growth steps. c_A is the equilibrium concentration of monomers. Mass conservation requires

$$c_A^0 = c_A + 2\sigma K {c_A}^2 + 3\sigma K^2 {c_A}^3 + ... + n\sigma K^{n-1} {c_A}^n$$

where c_A^0 is the total concentration of A in monomer form. Using the definition

$$s = Kc_A$$

this series can be written as

$$c_A^0 = c_A[1 + \sigma \sum_{j=2}^{n} j s^{j-1}] = c_A\left[1 - \frac{\sigma(s^2 - 2s + s^n(1 + n - sn))}{(s-1)^2}\right]$$

The degree of dissociation, α, defined as

$$\alpha = \frac{c_A}{c_A^0}$$

denotes the mole fraction of monomers referred to the total concentration of c_A^0, measured in monomer units. For a given set of parameters K, σ, and n, the degree of dissociation, α, and the heat of dissociation per injection, δh_i, can be calculated and can be compared with the experimental result. The partition function, Q, of the aggregation model is defined as

$$Q = 1 + \sigma(s + s^2 + ... + s^{n-1}) = 1 + \sigma \sum_{j=1}^{n-1} s^j = 1 - \frac{\sigma(s - s^n)}{s - 1}$$

and can be used to derive other properties of the system. For example, the probability of occurrence of an aggregate of size k is

$$p_k = \sigma s^{k-1}/Q$$

and the average aggregate size is given by

$$n_{av} = [1 + \sigma \sum_{j=1}^{n-1} (j+1) s^j]/Q$$

where n is the maximum aggregation number.

The solid lines in Figure 5b,c are theoretical results of the aggregation model calculated with the parameters $K = 1$/cmc, σ, and n listed in Table 3. The parameter σ determines the steepness of the monomer → aggregate transition and thus also the length of the plateau region for which the degree of dissociation is $\alpha = 1$. A small nucleation parameter makes nucleation difficult and extends the length of the monomer region.

As an obvious difference to the mass action model, the aggregation model predicts small heat changes even after the cmc is reached. In evaluations based on the mass action model this "tail" of the titration curve is often subtracted. In contrast, the aggregation model provides a quantitative explanation for this "tailing-off" behavior. The model predicts a small, but distinct heat uptake (~300 μcal per injection) even if the detergent concentration in the calorimeter cell is larger than the cmc (cf. Figure 5). In molecular terms this suggests small changes relating to the size, shape, and the degree of counterion condensation of the micelles.

Table 3 summarizes the fit parameters for DTAC and DeTAC. The nucleation parameter σ, which determines the sharpness of the transition, is constant with $\sigma = 10^{-4}$. The aggregation number n is 40−60 and is the minimum aggregation size to fit the experimental data. An increase of n beyond this limit produces only minor changes in the fit of the demicellization curve.

Figure 7 illustrates additional features of the cooperative aggregation model calculated with the same set of parameters as used to fit the experimental data in Figure 5. Figure 7a shows a semilogarithmic plot of the monomer equilibrium concentration c_A versus the total monomer concentration c_A^0 in the measuring cell. c_A increases steeply up to the cmc (i.e., linearly with c_A^0 in a nonlogarithmic plot) and then continues to increase with a much smaller gradient. In contrast to classical models, the monomer concentration c_A is not constant once the cmc is reached.

Figure 7b displays the average aggregate size, n_{aver}, plotted as a function of the total concentration c_A^0. The figure reveals a broad transition as the equilibrium concentration c_A varies only slowly with c_A^0 beyond the cmc. The average aggregate size at a total concentration of $c_A^0 = 100$ cmc is $n_{aver} = 27$. Literature data for the micellar size of DTAC vary in the range of $20 \leq n \leq 60$[8].

It is further possible to calculate the probabilities of aggregate of size i, p_i, and the mole fraction of monomers, α. This is illustrated in Figure 7c. At a monomer equilibrium concentration of $c_A = 15$ mM the calculated probabilities are $p_1 = 10^{-8}$, $p_{44} = 0.215$, and $p_{45} = 0.313$. Together the two largest aggregates account for more than 50% of all aggregates.

The cmc's of n-alkyl-trimethylammonium chlorides have been investigated before.[8,23−26] A systematic difference is noted between the present results and the standard analysis where ΔH^0_{demic} is evaluated by the distance between the two nearly horizontal regions in the ITC diagram (cf. Figure 5 in ref 23). The ΔH^0_{demic} values determined by the latter method are consistently ~10% smaller than the results obtained by the cooperative aggregation model.

Concluding Remarks

The cationic and anionic detergents investigated in this study show distinct differences in their interaction with lipid membranes. At a given length of the alkyl chain the

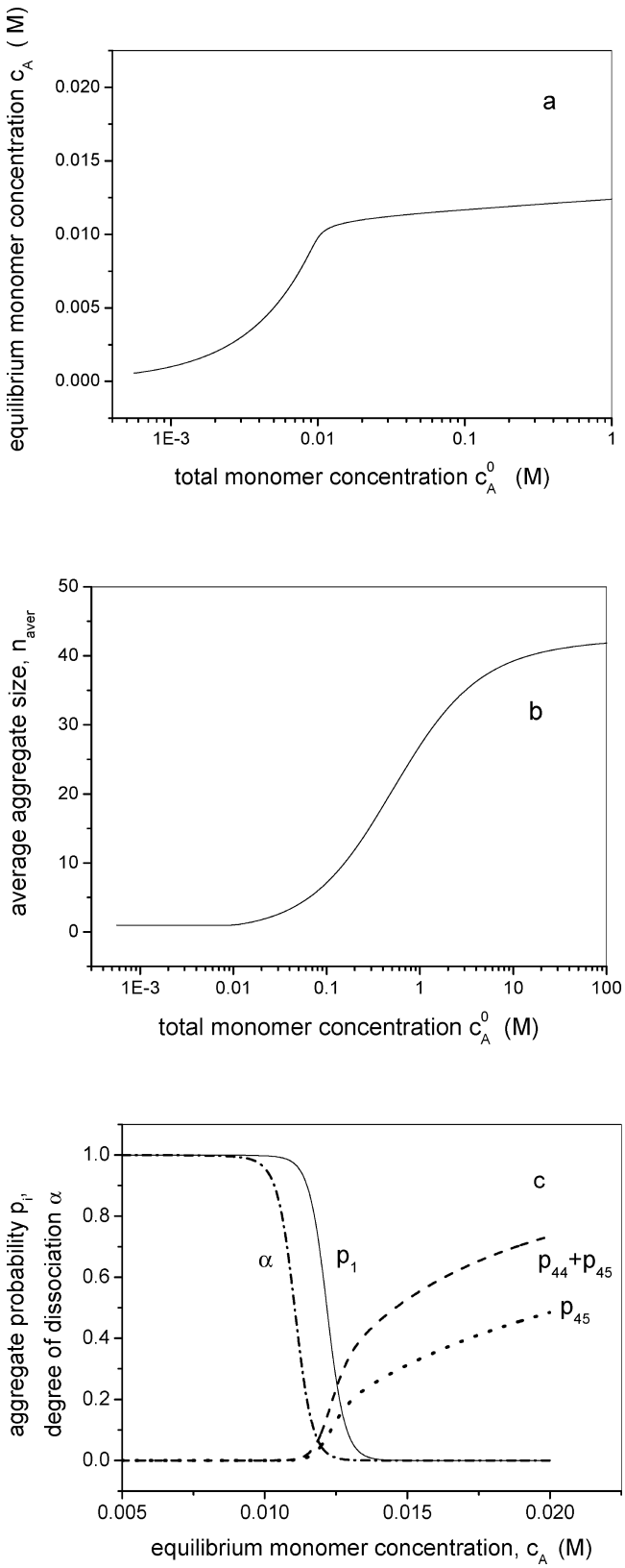

Figure 7. Cooperative aggregation model. Parameters identical to those used to fit the experimental data in Figure 5. $K = 97\ M^{-1}$, $\sigma = 10^{-4}$, $n = 45$. (a) Monomer equilibrium concentration c_A as a function of the total monomer concentration c_A^0 (semilogarithmic plot). c_A increases rapidly until the cmc (10.3 mM) is reached and then increases only slowly. (b) The average aggregation size, n_{aver}, as a function of the total monomer concentration, c_A^0. (c) p_i denotes the probability of aggregates of size i as a function of the monomer equilibrium concentration, c_A.

detergents with the $-SO_4^-$ headgroup bind better by a factor of 10−20 than those with the $^{+}N(CH_3)_3$ polar group. This can be traced back to two effects: (i) minimum repulsion and steric effects of the SO_4^- group in the membrane and (ii) maximum interaction of the alkyl chains in the membrane. In contrast, the $^{+}N(CH_3)_3$ polar group makes a positive (repulsive) contribution of 2.5 kcal/mol to membrane binding and reduces the packing of the hydrocarbon chains. The experiments demonstrate that the free energy contributions of head and tail are not really decoupled as suggested previously. The n-alkyl-sulfates dissolve membranes already at low bound detergent-to-lipid ratios; n-alkyl-trimethylammonium salts can be integrated into bilayer membranes up to very high concentrations, which may explain, in part, their increased biological toxicity.

Acknowledgment. This work was supported by the Swiss National Science Foundation Grant No. 31003A-129701/1.

References and Notes

(1) Hope, M. J.; Bally, M. B.; Webb, G.; Cullis, P. R. *Biochim. Biophys. Acta* **1985**, *812*, 55.

(2) Mayer, L. D.; Hope, M. J.; Cullis, P. R. *Biochim. Biophys. Acta* **1986**, *858*, 161.

(3) Gerebtzoff, G.; Li-Blatter, X.; Fischer, H.; Frentzel, A.; Seelig, A. *ChemBioChem* **2004**, *5*, 676.

(4) Seelig, J.; Nebel, S.; Ganz, P.; Bruns, C. *Biochemistry* **1993**, *32*, 9714.

(5) Heerklotz, H.; Seelig, J. *Biochim. Biophys. Acta* **2000**, *1508*, 69.

(6) Tanford, C. The hydrophobic effect. *Formation of micelles and biological membranes*, 2nd ed.; Wiley: New York, 1980.

(7) Lichtenberg, D.; Robson, R. J.; Dennis, E. A. *Biochim. Biophys. Acta* **1983**, *737*, 285.

(8) Beyer, K.; Leine, D.; Blume, A. *Colloids Surf., B* **2006**, *49*, 31.

(9) Aveyard, R.; Haydon, D. A. *An introduction to the principles of surface chemistry*; Cambridge University Press: London, 1973.

(10) McLaughlin, S. *Curr. Top. Membr. Transp.* **1977**, 71.

(11) Tan, A.; Ziegler, A.; Steinbauer, B.; Seelig, J. *Biophys. J.* **2002**, *83*, 1547.

(12) Cantor, C. R.; Schimmel, P. R. *Biophysical Chemistry*; Freeman: San Francisco, 1980; Vol. I.

(13) Hanakam, F.; Gerisch, G.; Lotz, S.; Alt, T.; Seelig, A. *Biochemistry* **1996**, *35*, 11036.

(14) Boguslavsky, V.; Rebecchi, M.; Morris, A. J.; Jhon, D. Y.; Rhee, S. G.; McLaughlin, S. *Biochemistry* **1994**, *33*, 3032.

(15) Seelig, A. *Biochim. Biophys. Acta* **1987**, *899*, 196.

(16) Meier, M.; Seelig, J. *Biophys. J.* **2010**, *98*, 1529.

(17) Heerklotz, H.; Seelig, J. *Biophys. J.* **2000**, *78*, 2435.

(18) Heerklotz, H.; Seelig, J. *Biophys. J.* **2001**, *81*, 1547.

(19) de la Maza, A.; Parra, J. L. *Biophys. J.* **1997**, *72*, 1668.

(20) Seelig, J.; Macdonald, P. M.; Scherer, P. G. *Biochemistry* **1987**, *26*, 7535.

(21) Heyn, M. P.; Bretz, R. *Biophys. Chem.* **1975**, *3*, 35.

(22) Robinson, B. H.; Löffler, A.; Schwarz, G. *J. Chem. Soc., Faraday Trans. 1* **1973**, *69*, 56.

(23) Chakraborty, I.; Moulik, S. P. *J. Phys. Chem. B* **2007**, *111*, 3658.

(24) Sarac, B.; Bester-Rogac, M. *J. Colloid Interface Sci.* **2009**, *338*, 216.

(25) Perger, T. M.; Bester-Rogac, M. *J. Colloid Interface Sci.* **2007**, *313*, 288.

(26) Zielinski, R. *J. Colloid Interface Sci.* **2001**, *235*, 201.

(27) Anatrace Catalogue, 2009/2010; Anatrace: Santa Clara, CA.

(28) Paula, S.; Sus, W.; Tuchtenhagen, J.; Blume, A. *J. Phys. Chem.* **1995**, *99*, 11742.

(29) Ranganathan, R.; Tran, L.; Bales, B. L. *J. Phys. Chem. B* **2000**, *104*, 2260.

JP107088D